

# Estimated Human Absorbed Dose of $^{111}\text{In}$ -BPAMD as a New Bone-Seeking SPECT-Imaging Agent

H. Yousefnia, S. Zolghadri

**Abstract**—An early diagnosis of bone metastasis is very important for making a right decision on a subsequent therapy. One of the most important steps to be taken initially, for developing a new radiopharmaceutical is the measurement of organ radiation exposure dose. In this study, the dosimetric studies of a novel agent for SPECT-imaging of the bone metastasis,  $^{111}\text{In}$ -(4-{{(bis(phosphonomethyl)carbamoyl)methyl}7,10bis(carboxymethyl)-1,4,7,10-tetraazacyclododec-1-yl) acetic acid ( $^{111}\text{In}$ -BPAMD) complex, have been carried out to estimate the dose in human organs based on the data derived from mice. The radiolabeled complex was prepared with high radiochemical purity in the optimal conditions. Biodistribution studies of the complex was investigated in the male Syrian mice at the selected times after injection (2, 4, 24 and 48 h). The human absorbed dose estimation of the complex was made based on data derived from the mice by the radiation absorbed dose assessment resource (RADAR) method.

$^{111}\text{In}$ -BPAMD complex was prepared with high radiochemical purity >95% (ITLC) and specific activities of 2.85 TBq/mmol. Total body effective absorbed dose for  $^{111}\text{In}$ -BPAMD was 0.205 mSv/MBq. This value is comparable to the other  $^{111}\text{In}$  clinically used complexes. The results show that the dose with respect to the critical organs is satisfactory within the acceptable range for diagnostic nuclear medicine procedures. Generally,  $^{111}\text{In}$ -BPAMD has interesting characteristics and it can be considered as a viable agent for SPECT-imaging of the bone metastasis in the near future.

**Keywords**—In-111, BPAMD, absorbed dose, RADAR.

## I. INTRODUCTION

**S**KELETAL metastases are the most common malignant tumors in the skeleton involving up to 70% of patients with prostate and breast cancers, and up to 30% of those with cancers of the lung, bladder, and thyroid [1], [2]. Imaging plays an important role in the detection, diagnosis, prognostication, treatment planning, and follow-up monitoring of the bone metastasis. Capturing images is of particular importance for a crucial decision on a subsequent therapy [3]. However,  $^{99\text{m}}\text{Tc}$ -methylene diphosphonate (MDP) is a well-established tracer for the diagnosis of the bone metastasis in nuclear medicine domain using SPECT imaging [4], but the search for developing new SPECT radiotracers can be especially important nowadays because of  $^{99\text{m}}\text{Tc}$  shortage. Nowadays, (4-{{(bis(phosphonomethyl)carbamoyl)methyl}-7,10-bis(carboxymethyl)-1,4,7,10-tetraazacyclododec-1-yl) acetic acid (BPAMD), as a new macrocyclic diphosphonate, has fulfilled some requirements and removed a number of restrictions of the first generation phosphonates, such as

EDTMP and HEDP. This complex, labeled with  $^{68}\text{Ga}$ , showed promising results such as very high target-to-soft-tissue ratios and ultrafast clearance [5].

The interesting physical properties of  $^{111}\text{In}$  [a cyclotron produced radionuclide with half-life of 2.8 days, decaying by electron capture (EC) with subsequent emission of gamma photons of 173 and 247 keV (89% and 94% intensity, respectively)] as well as its easy production and availability, make it an interesting nuclide for radiopharmaceutical research. Various carriers including bombesin [6], immunoglobulins [7] and HlgG [8] labeled with  $^{111}\text{In}$  have shown the usefulness of this radioisotope in the detection and diagnosis of infections and inflammatory lesions using single photon emission computed tomography (SPECT).

The amount of energy is deposited in any organs by ionizing radiation termed absorbed dose, plays an important role in evaluating the risks associated with the administration of radiopharmaceuticals and thus the maximum amount of activity that should be undertaken [9]. Many resources for facilitating dose calculations are available, once appropriate biokinetic data are gathered in animal or human experiments [10]. In nuclear medicine, the most commonly used method these days for calculation of the internal absorbed dose estimates is the radiation dose assessment resource (RADAR) method [11].

In this research, the human absorbed dose of  $^{111}\text{In}$ -BPAMD complex, as a possible SPECT imaging agent for the bone metastasis was estimated based on the data taken from the Syrian mice type by RADAR method.

## II. MATERIALS AND METHODS

The enriched cadmium-112 with purity of >99% was obtained from Merck (Darmstadt, Germany). BPAMD was prepared from ABX (Radeberg, Germany). All other chemical reagents were purchased from Sigma-Aldrich (Heidelberg, Germany). Whatman No. 2 paper was provided from Whatman (Buckinghamshire, U.K.). 30 MeV cyclotron (Cyclone 30, IBA, Belgium) was used for the production of  $^{111}\text{In}$  via  $^{112}\text{Cd}(p,2n)^{111}\text{In}$  reaction. Radio-chromatography and imaging studies were performed using a thin layer chromatography scanner (Bioscan AR2000, Paris, France) and a Dual Head SPECT system (DST-XL, SMV, Buc, France). The activity of the samples was measured by a p-type coaxial high-purity germanium (HPGe) detector (EGPC 80-200R) coupled with a multichannel analyzer card system (GC1020-7500SL, Canberra, U. S. A.). Calculations were based on the 172 keV peak for  $^{111}\text{In}$ . All values were expressed as mean  $\pm$  standard deviation (Mean  $\pm$  SD) and the data were compared

H. Yousefnia and S. Zolghadri are with the Nuclear Science and Technology Research Institute (NSTRI), Tehran, Iran (e-mail: hyousefnia@aeoi.org.ir, szolghadri@aeoi.org.ir).

using student T-test. Statistical significance was defined as  $P < 0.05$ . Animal studies were conducted in accordance with the United Kingdom Biological Council's Guidelines on the Use of Living Animals in Scientific Investigations, second edition.

#### A. Production and Quality Control of $^{111}\text{InCl}_3$ Solution

In order to prepare Cd targets for the production, cadmium electroplating was performed on a copper surface. Indium-111 chloride was prepared by 22 MeV proton bombardment of the cadmium target at a 30 MeV cyclotron, with a current of 100  $\mu\text{A}$  for 48 min (80  $\mu\text{Ah}$ ). Indium-111 was eluted with 1 N HCl (25 mL) as  $^{111}\text{InCl}_3$  for labeling use. Radionuclidic purity of the final solution was carried out by counting in an HPGe detector for 1000 seconds. The concentrations of cadmium (from target material) and copper (from target support) were determined using polarography. The radiochemical purity of the  $^{111}\text{InCl}_3$  solution was checked by instant thin layer chromatography method (ITLC) in two solvent systems, 1 mM DTPA and 10% ammonium acetate:methanol mixture.

#### B. Preparation and Quality Control of $^{111}\text{In-BPAMD}$

In order to obtain maximum labeling yield, several experiments were carried out by the variation of different reaction parameters. In the optimal procedure, 1 mg of BPAMD was dissolved in 1 mL pure water and the aqueous solution was used for labeling studies. 75  $\mu\text{L}$  (130 nmol) of the stock solution was added to the vial containing 370 MBq of  $^{111}\text{InCl}_3$ . The pH of the reaction mixture was adjusted to 6 and the mixture was incubated for 60 min at 100  $^\circ\text{C}$ . Different chromatographic systems were used for the detection of the radiolabeled compound from the free indium cation.  $\text{NH}_4\text{OH}:\text{MeOH}:\text{H}_2\text{O}$  (0.2:2:4) solvent system was considered as the best ITLC mobile phase.

#### C. Biodistribution of Radiolabeled Complex in Syrian Mice

100  $\mu\text{L}$  of final  $^{111}\text{In-BPAMD}$  solution with approximately 3.7 MBq radioactivity (pH 7) was injected intravenously into the male Syrian mice through their tail veins. The total amount of radioactivity injected into each animal was measured by counting the 1-mL syringe before and after injection in a dose calibrator with fixed geometry. The biodistribution of the solutions among tissues were determined by scarification of 5 mice with around 18 weeks old for each selected interval time (2, 4, 24 and 48 h) after injection under the animal care protocols.

Blood samples were rapidly taken after scarification. The tissues (the skin, heart, kidneys, spleen, stomach, intestine, bone, muscle, lung and liver) were weighed and rinsed with normal saline and their activities were determined with a p-type coaxial HPGe detector coupled with a multichannel analyser according to (1) [12]:

$$A = \frac{N}{\epsilon \gamma t_s m k_1 k_2 k_3 k_4 k_5} \quad (1)$$

where,  $\epsilon$  is the efficiency at photopeak energy,  $\gamma$  is the emission probability of the gamma line corresponding to the

peak energy,  $t_s$  is the live time of the sample spectrum collection in seconds,  $m$  is the mass (kg) of the measured sample,  $k_1$ ,  $k_2$ ,  $k_3$ ,  $k_4$  and  $k_5$  are the correction factors for the nuclide decay from the time the sample is collected to start the measurement, the nuclide decay during counting period, self-attenuation in the measured sample, pulses loss due to random summing and the coincidence, respectively.  $N$  is the corrected net peak area of the corresponding photopeak given as:

$$N = N_s \frac{t_s}{t_b} N_b \quad (2)$$

where  $N_s$  is the net peak area in the sample spectrum,  $N_b$  is the corresponding net peak area in the background spectrum and  $t_b$  is the live time of the background spectrum collection in seconds.

The percentage of injected dose per gram (%ID/g) for different organs was calculated by dividing the activity amount of each tissue (A) to the decay-corrected injected activity and the mass of each organ. Five mice were sacrificed for each time interval. All values were expressed as mean  $\pm$  standard deviation and the data were compared using Student's T-test.

#### D. Calculation of Accumulated Activity in Human Organs

The accumulated source activity for each animal organ was calculated according to (3), where A (t) is the activity of each organ at time t.

$$\bar{A} = \int_{t_1}^{\infty} A(t) dt \quad (3)$$

For this purpose, the data points, which represent the non-decay corrected percentage-injected dose, were created. A linear approximation was used between the two experimental points of times. The curves were extrapolated to infinity by fitting the tail of each curve to a monoexponential curve with the exponential coefficient equal to the physical decay constant of  $^{111}\text{In}$ . Whereas, the activity of blood at  $t=0$  was considered as the total amount of injected activity, the activity of the all other organs was estimated to be zero at that time. The accumulated activity was calculated by computing the area under the curves.

The accumulated activity in the animals was extrapolated to the accumulated activity in humans by the proposed method of Sparks et al. (4) [13]:

$$\bar{A}_{human\ organ} = \bar{A}_{human\ organ} \times \frac{\text{Organ Mass}_{human} / \text{Body Mass}_{human}}{\text{Organ Mass}_{animal} / \text{Body Mass}_{animal}} \quad (4)$$

In order to extrapolate this accumulated activity to human, the standard mean weight of each organ for human was used [14].

#### E. Equivalent Absorbed Dose Calculation

The absorbed dose in the human organs was calculated by RADAR formalism based on the biodistribution data in the mice [11]:

$$D = \tilde{A} \times DF \quad (5)$$

where  $\tilde{A}$  is the accumulated activity for each human organ, and DF is:

$$DF = \frac{k \sum_i n_i E_i \phi_i}{m} \quad (6)$$

In (6),  $n_i$  is the number of radiations with the energy  $E$  emitted per nuclear transition,  $E_i$  is the energy per radiation (MeV),  $\phi_i$  is the fraction of energy emitted that is absorbed in the target,  $m$  is the mass of the target region (kg) and  $k$  is some proportionality constant ( $\frac{\text{mGy.kg}}{\text{MBq.s.MeV}}$ ). DF represents the physical decay characteristics of the radionuclide, the range of the emitted radiations, and the organ size and configuration [15] expressed in mGy/MBq.s. In this research, DFs have been taken from the amount presented in OLINDA/EXM software [11].

Since  $D$  in (5) is the absorbed dose in the target organ directly from a source organ, the total absorbed dose for each target organ was computed by the summation of the absorbed dose delivered from each source organ.

#### F. Effective Absorbed Dose Calculation

The effective absorbed dose for each organ was computed by (7)

$$E = \sum_T W_T H_T \quad (7)$$

where  $H_T$  is the equivalent absorbed dose for each organ and  $W_T$  is the tissue-weighting factor which represents a subjective balance between the different stochastic health risks [16].  $W_T$  was obtained from the reported value in ICRP 103 [17].

### III. RESULTS

#### A. Radionuclide Production

$^{111}\text{In}$ , in the form of  $\text{InCl}_3$ , was prepared by 22 MeV proton bombardment of the enriched  $^{112}\text{Cd}$  target at Cyclone-30. Radionuclidic control showed the presence of 173 and 247 keV gamma energies, all originating from  $^{111}\text{In}$  that indicated the radionuclidic purity of higher than 99%. The concentrations of cadmium (from target material) and copper (from target support) determined by polarography, showed to be below the internationally accepted levels, i.e. 0.1 ppm for Cd and Cu [18], [18, p 1895].

The radiochemical purity of the  $^{111}\text{In}$  solution was checked using Whatman No.2 paper in two solvent systems. In 1 mM DTPA solution, free  $\text{In}^{3+}$  cation is converted to the  $\text{In-DTPA}$  form (the more lipophilic form than free  $\text{In}^{3+}$  cation) and migrates to the higher  $R_f$  (0.8). Any other  $\text{In}$  ionic species in the solution such as  $\text{InCl}_4^-$  or colloids, do not form a complex with DTPA and therefore in the presence of these ionic species, small radioactive fraction would be observed at the origin (not seen in this experiment). In the case of 10% ammonium acetate:methanol mixture,  $\text{In}^{3+}$  and/or colloids remain at  $R_f=0.1$ , whereas, the other ionic  $^{111}\text{In}$  species would elute faster and migrate to higher  $R_f$  (not seen in this experiment).

#### B. Preparation and Quality Control of $^{111}\text{In-BPAMD}$

ITLC studies confirmed the production of  $^{111}\text{In-BPAMD}$  in 60 min with above 95% radiochemical purity; the remaining is possibly attributed to other  $\text{In}$  ionic species which cannot react with BPAMD or the colloids. Since in the  $\text{NH}_4\text{OH}:\text{MeOH}:\text{H}_2\text{O}$  (0.2:2:4) solvent system, the free indium remains at the origin of the paper as a single peak, while the radiolabeled compound migrates to higher  $R_f$  (0.7) (Fig. 1), this mobile phase can also be distinguished between the colloids and  $^{111}\text{In-BPAMD}$ .

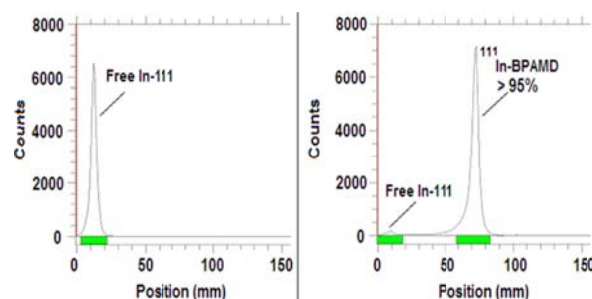


Fig. 1 ITLC of  $^{111}\text{InCl}_3$  (left) and  $^{111}\text{In-BPAMD}$  (right) in  $\text{NH}_4\text{OH}:\text{MeOH}:\text{H}_2\text{O}$  (0.2:2:4) solution on Whatman No.2 papers

#### C. Biodistribution of Radiolabeled Complex in Syrian Mice

The percentage of the injected dose per gram in mice organs up to 48 h after injection of the radiolabeled complexes was determined. The non-decay corrected clearance curves from the main organ sources of the mice for  $^{111}\text{In-BPAMD}$  are shown in Fig. 2. As expected, the major portion of the injected radioactivity remaining in the body is transferred from the blood circulation into the bones for both complexes. The radioactivity uptake in the bone is enhanced with time up to 4 h after injection. Also, the significant excretion of the radioactivity is observed in the kidneys showing the major route of excretion for the labeled compound is through the urinary tract.

#### D. Dosimetric Studies

Dosimetric evaluation in human organs was carried out by RADAR method based on biodistribution data in the mice organs. The equivalent and effective absorbed dose in human organs after intravenously injection of  $^{111}\text{In-BPAMD}$  are presented in Table I. The total body effective absorbed dose for  $^{111}\text{In-BPAMD}$  is 0.205 mSv/MBq.

### IV. DISCUSSION

The ability to capture an image from an organ is considerably dependent on the concentration of the radiopharmaceutical in the organ of interest. Actually, images with better contrast can be obtained for tracers with higher target/non-target uptake ratio [19]. Specific uptake and retention in the target organ and rapid clearance from non-target organs are significant parameters for the ideal SPECT tracer [20].

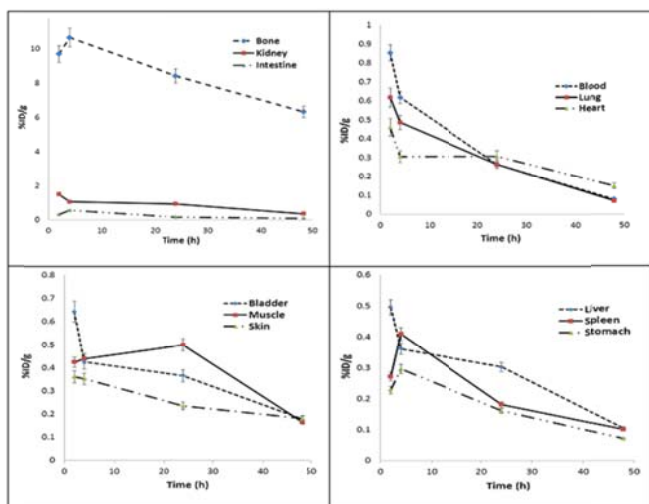


Fig. 2 Non-decay corrected clearance curves for each organ of Syrian mice after intravenously injection of  $^{111}\text{In}$ -BPAMD

TABLE I  
 EQUIVALENT AND EFFECTIVE ABSORBED DOSE DELIVERED INTO HUMAN  
 ORGANS AFTER INJECTION OF  $^{111}\text{In}$ -BPAMD

Target Organs	Equivalent absorbed dose (mSv/MBq)	$W_t^a$	Equivalent absorbed dose (mSv/MBq)
Adrenals	0.092	0.12	0.011
Brain	0.097	0.01	0.001
Breasts	0.029	0.12	0.003
GB Wall	0.042	0.12	0.050
LLI Wall	0.075	0.12	0.009
Small Int	0.051	0.12	0.006
Stomach Wall	0.038	0.12	0.005
ULI Wall	0.044	0.12	0.005
Heart Wall	0.058	0.12	0.007
Kidneys	0.068	0.12	0.008
Liver	0.050	0.04	0.002
Lungs	0.060	0.12	0.003
Muscle	0.068	0.12	0.008
Ovaries	0.059	0.08	0.005
Pancreas	0.058	0.12	0.007
Red Marrow	0.334	0.12	0.040
Bone Surf	0.860	0.01	0.009
Spleen	0.049	0.12	0.006
Testes	0.037	0.12	0.004
Thymus	0.045	0.12	0.005
Thyroid	0.065	0.04	0.003
UB Wall	0.039	0.04	0.002
Uterus	0.046	0.12	0.006
Total Body	0.131		0.205

According to the importance of the target and non-target organs uptakes in the quality of images, and furthermore, in the unnecessary radiation exposure to the patients, biodistribution studies after intravenous injection of  $^{111}\text{In}$ -BPAMD to the male Syrian mice were surveyed. Based on the obtained results, it is clearly concluded that the major portion of the injected activity of the complex is transferred from the blood circulation to the bones. The significant excretion of the radioactivity is observed in the kidneys as anticipated due to the water solubility of the compound, the major route of

excretion for the labeled compound is through the urinary tract. It goes without saying that, the liver plays no significant role in the metabolism of the both complexes.

A prerequisite for the clinically application of a new diagnostic radiopharmaceutical is the measurement of organ radiation exposure dose from the biodistribution data in animals [21]. These results can be used to estimate the maximum permissible administered activity which maintains the organ doses within an acceptable range. Minimizing the radiation exposure to the patients while providing scintigraphic images with good quality, is the key point which should be considered.

In this study, the radiation absorbed dose of a new  $^{111}\text{In}$  bone seeking agent in human organ was calculated based on the biodistribution data as regards the Syrian mice. Calculation of the radiopharmaceuticals absorbed dose in human organs from biodistribution in small animals can be useful for determining the injected activity and accelerating the development of radioactive compounds to be used in clinical settings, and is a common initial step, consistent with the recommendations of ICRP 62 [22]. The equivalent and effective absorbed dose in human organs after intravenous injection of  $^{111}\text{In}$ -BPAMD are presented in Table I. The dose received to the critical organs is well within the acceptable considered range for diagnostic nuclear medicine procedures [22], [23].

A comparison between the absorbed doses of the new radiolabeled complex with the other  $^{111}\text{In}$  clinically used radiopharmaceuticals indicates that the novel product is advantageous. The total body effective dose of the adult after injection of  $^{111}\text{In}$  labeled platelets,  $^{111}\text{In}$  labeled red blood cells and  $^{111}\text{In}$  labeled WBC's are 0.52, 0.20 and 0.67 mSv/MBq, respectively [24]. This value is much less in  $^{111}\text{In}$ -BPAMD. The difference can be related to the fast clearance of the new bone-seeking agent and also the low amounts of the non-target organs uptake and can be considered as a remarkable benefit.

#### V. CONCLUSION

$^{111}\text{In}$ -BPAMD was prepared with high radiochemical purity and specific activities of 2.85 TBq/mmol. Biodistribution studies of the complex performed in the Syrian mice, showed major accumulation of the labelled compound in the bone tissue, while the other tissues uptakes were almost negligible. The total body effective absorbed dose for  $^{111}\text{In}$ -BPAMD is 0.205 mSv/MBq, which is comparable to the other  $^{111}\text{In}$  clinically used complexes. The dose received to the critical organs for the complex is well within the acceptable considered range for diagnostic nuclear medicine procedures. The results show that  $^{111}\text{In}$ -BPAMD has interesting characteristics and it can be considered as a viable agent for SPECT-imaging of the bone metastasis.

#### ACKNOWLEDGMENT

The authors wish to thank Nuclear Sciences and Technology Research Institute (NSTRI) for financial supports

REFERENCES

- [1] IAEA-TECDOC-1549, "Criteria for Palliation of Bone Metastases-Clinical Applications," Austria, Vienna: IAEA; 2007.
- [2] A. Lipton, "Pathophysiology of Bone Metastases: How This Knowledge May Lead to Therapeutic Intervention," *J. Support. Oncol.* vol. 2, pp. 205-20, 2004.
- [3] M. Fellner, B. Biesalski, N. Bausbacher, V. Kubicek, P. Hermann, F. Rösch, O. Thews, "<sup>68</sup>Ga-BPAMD: PET-imaging of bone metastases with a generator based positron emitter," *Nucl. Med. Biol.* vol. 39, pp. 993-9, 2012.
- [4] G. Zettinig, T. Leitha, B. Niederle, K. Kaserer, A. Becherer, K. Kletter, et al. "FDG positron emission tomographic, radioiodine, and MIBI imaging in a patient with poorly differentiated insular thyroid carcinoma," *Clin. Nucl. Med.* Vol. 26, pp. 599-601, 2001.
- [5] H. Yousefnia, A.R. Jalilian, S. Zolghadri, A. Mirzaei, A. Bahrami-Samani, M. Mirzaei, M. Ghannadi, "Development of <sup>111</sup>In DOTMP for dosimetry of bone pain palliation agents," *J. Radioanal. Nucl. Chem.* DOI 10.1007/s10967-014-3911-6.
- [6] M. Fellner, R.P. Baum, V. Kubicek, P. Hermann, I. Lukeš, V. Prasad et al., "PET/CT imaging of osteoblastic bone metastases with <sup>68</sup>Ga-bisphosphonates: first human study," *Eur. J. Nucl. Med. Mol. Imaging*, vol. 37, pp. 834, 2010.
- [7] J. Lai, S.M. Quadri, P.E. Borchardt, L. Harris, R. Wucher, E. Askew et al., "Pharmaco-kinetics of radiolabeled polyclonal antiferritin in patients with Hodgkin's disease," *Clin. Cancer Res.* vol. 5, pp. 3315-23, 1999.
- [8] M.W. Nijhof, W.J. Oyen, A. Van Kampen, R.A. Claessens, J.W. Van der Meer, F.H. Corstens, "Evaluation of infections of the locomotor system with indium-111-labeled human IgG scintigraphy," *J. Nucl. Med.*, vol. 38, pp. 1300-05, 1997.
- [9] M.G. Stabin, M. Tagesson, S.R. Thomas, M. Ljungberg, S.E. Strand, "Radiation dosimetry in nuclear medicine," *Appl. Radiat. Isot.*, vol. 50, pp. 73-87, 1996.
- [10] M.G. Stabin, "Internal Dosimetry in Nuclear Medicine," *Braz. J. Radiat. Sci.*, vol. 01, pp. 1-15, 2013.
- [11] M.G. Stabin, J.A. Siegel, "Physical Models and Dose Factors for Use in Internal Dose Assessment," *Health. Phys.*, vol. 85, pp. 294-310, 2003.
- [12] IAEA-TECDOC-1401, "Quantifying uncertainty in nuclear analytical measurements," Austria, Vienna: IAEA; 2004.
- [13] R.B. Sparks, B. Aydogan, "Comparison of the effectiveness of some common animal data scaling techniques in estimating human radiation dose," *Sixth International Radiopharmaceutical Dosimetry Symposium*, Oak Ridge, TN: Oak Ridge Associated Universities, pp. 705-16, 1996.
- [14] H. Yousefnia, S. Zolghadri, A.R. Jalilian, M. Tajik, M. Ghannadi-Maragheh, "Preliminary dosimetric evaluation of <sup>166</sup>Ho-TTHMP for human based on biodistribution data in rats," *Appl. Radiat. Isot.*, vol. 94, pp. 260-5, 2014.
- [15] J.J. Bevelacqua, "Internal dosimetry primer," *Radiat. Prot. Manage.*, vol. 22, pp. 7-17, 2005.
- [16] D.J. Brenner, "Effective dose: a flawed concept that could and should be replaced," *British. J. Radiol.*, vol. 81, pp. 521-3, 2008.
- [17] ICRP Publication 103, "The 2007 Recommendations of the International Commission on Radiological Protection," *Ann. ICRP*, vol. 37, pp. 2-4, 2007.
- [18] United States Pharmacopoeia 28, NF 23, pp. 1009, 2005.
- [19] J.T. Bushberg, J.A. Seibert, E.M. Leidholdt, J.M. Boone, "The Essential Physics of Medical Imaging," Third Edition, Lippincott Williams & Wilkins; 2011.
- [20] C. Muller, R. Schibli, "Single Photon Emission Computed Tomography Tracer," *Mol. Imaging Oncol.* vol. 187, pp. 65-105. 2013.
- [21] A.L. Kesner, W.A. Hsueh, J. Czernin, H. Padgett, M.E. Phelps, D.H. Silverman, "Radiation dose estimates for (<sup>18</sup>F)5-fluorouracil derived from PET-based and tissue-based methods in rats," *Mol. Imaging Biol.*, vol. 10, pp. 341-8, 2008.
- [22] ICRP Publication 62, "Radiological Protection in Biomedical Research," *Ann. ICRP*, vol. 22, pp. 3, 1993.
- [23] ICRP Publication 53, "Radiation Dose to Patients from Radiopharmaceuticals," *Ann. ICRP*, vol. 18, pp. 1-4, 1988.
- [24] Radiation Internal Dose Information Center, "Radiation dose estimates to adults and children from various radiopharmaceuticals," Oak Ridge Institute for Science and Education. Oak Ridge, TN 37831. Available at: [orise.orau.gov/files/reacts/pedose.pdf](http://orise.orau.gov/files/reacts/pedose.pdf).